Monthly Notices
of the
ROYAL ASTRONOMICAL SOCIETY

Mon. Not. R. Astron. Soc. **400,** 258–262 (2009) doi:10.1111/j.1365-2966.2009.15445.x

The first broad-band X-ray study of the Supergiant Fast X-ray Transient SAX J1818.6−1703 in outburst

L. Sidoli,[1⋆] P. Romano,[2] P. Esposito,[1,3] V. La Parola,[2] J. A. Kennea,[4] H. A. Krimm,[5,6] M. M. Chester,[4] A. Bazzano,[7] D. N. Burrows[4] and N. Gehrels[5]

[1]*INAF, Istituto di Astrofisica Spaziale e Fisica Cosmica, Via E. Bassini 15, I-20133 Milano, Italy*
[2]*INAF, Istituto di Astrofisica Spaziale e Fisica Cosmica, Via U. La Malfa 153, I-90146 Palermo, Italy*
[3]*INFN, Sezione di Pavia, Via A. Bassi 6, I-27100 Pavia, Italy*
[4]*Department of Astronomy and Astrophysics, Pennsylvania State University, University Park, PA 16802, USA*
[5]*NASA/Goddard Space Flight Center, Greenbelt, MD 20771, USA*
[6]*Universities Space Research Association, Columbia, MD, USA*
[7]*INAF, Istituto di Astrofisica Spaziale e Fisica Cosmica, Via Fosso del Cavaliere 100, I-00133 Roma, Italy*

Accepted 2009 July 22. Received 2009 July 21; in original form 2009 June 19

ABSTRACT

The Supergiant Fast X-ray Transient (SFXT) SAX J1818.6−1703 underwent an outburst on 2009 May 6 and was observed with *Swift*. We report on these observations which, for the first time, allow us to study the broad-band spectrum from soft to hard X-rays of this source. No X-ray spectral information was available on this source before the *Swift* monitoring. The spectrum can be deconvolved well with models usually adopted to describe the emission from HMXB X-ray pulsars, and is characterized by a very high absorption, a flat power law (photon index ∼0.1–0.5) and a cut-off at about 7–12 keV. Alternatively, the SAX J1818.6−1703 emission can be described with a Comptonized emission from a cold and optically thick corona, with an electron temperature $kT_{\rm e} = 5$–7 keV, a hot seed photon temperature, kT_0, of 1.3–1.4 keV and an optical depth for the Comptonizing plasma, τ, of about 10. The 1–100 keV luminosity at the peak of the flare is 3×10^{36} erg s^{-1} (assuming the optical counterpart distance of 2.5 kpc). These properties of SAX J1818.6−1703 resemble those of the prototype of the SFXT class, XTE J1739–302. The monitoring with *Swift*/XRT reveals an outburst duration of about 5 d, similar to other members of the class of SFXTs, confirming SAX J1818.6−1703 as a member of this class.

Key words: X-rays: binaries – X-rays: individual: SAX J1818.6−1703.

1 INTRODUCTION

Supergiant Fast X-ray Transients (SFXTs) are transient X-ray sources in binary systems composed of a compact object and a blue supergiant companion. Although some of them were discovered before the *INTEGRAL* satellite launch in 2002, this new class of high mass X-ray binaries (HMXBs) was recognized only after several new peculiar X-ray transients had been discovered as a result of the Galactic plane survey performed by *INTEGRAL* (Sguera et al. 2005; Negueruela et al. 2006). The members of this new class of sources (about 10, with ∼20 candidates) display apparently short outbursts (as observed with *INTEGRAL*), characterized by a few hour duration flares and by a high dynamic range (1000–100 000) between the quiescence (10^{32} erg s^{-1}) and the flare peak (10^{36}–10^{37} erg s^{-1}). Spectral properties are very similar to those of HMXB pulsars (Romano et al. 2008).

Their long-term X-ray properties have been investigated thanks to a monitoring campaign with *Swift* (still ongoing, see Romano et al. 2009b), which is unveiling several new properties of a sample of SFXTs. This *Swift* campaign has demonstrated that the SFXTs short flares are part of a longer outburst phase lasting for days (Sidoli et al. 2009b), and they spend most of their lifetime in accretion at an intermediate level (10^{34} erg s^{-1}), instead of staying in quiescence (as was previously thought; Sidoli et al. 2008). The actual mechanism responsible for the outbursts is still unknown (see Sidoli 2009 for a review of the different proposed scenarios).

SAX J1818.6−1703 is an X-ray source classified as a SFXT because of its transient X-ray activity, its high dynamic range (Bozzo et al. 2008) and its association with a blue supergiant star located at 2.5 kpc (O9–B1 type; Negueruela & Smith 2006; Negueruela & Schurch 2007), thanks to the subarcsecond X-ray position obtained using *Chandra* (in't Zand et al. 2006). SAX J1818.6−1703 was discovered with the wide field cameras on board *BeppoSAX* (in't Zand et al. 1998), and showed several more bright flares lasting 1–3 h as observed with IBIS/ISGRI on board *INTEGRAL* (Grebenev

⋆E-mail: sidoli@lambrate.inaf.it

& Sunyaev 2005; Sguera et al. 2005), reaching ∼200 mCrab at the flare peak (18–45 keV), and with ASM on board *RXTE* (Sguera et al. 2005). Further and more recent activity has been caught both by *Swift*/BAT (Barthelmy et al. 2008) and by *INTEGRAL* (Grebenev & Sunyaev 2008). A periodicity (likely orbital) of 30 d was discovered (Bird et al. 2009; Zurita Heras & Chaty 2009) from the analysis of available *Swift*/BAT and *INTEGRAL* data, suggesting an eccentric orbit ($e \sim 0.3$–0.4) and an outburst duration of around 4 to 6 days.

Here, we report on the latest outburst from this source, observed with *Swift* starting on 2009 May 6 (Romano et al. 2009d). These *Swift* observations allow us to perform the first broad-band spectroscopy of this SFXT, simultaneously from soft to hard X-rays.

2 OBSERVATIONS AND DATA REDUCTION

SAX J1818.6−1703 triggered the *Swift*/BAT three times since the start of the mission, on 2007 October 16 at 04:20:16 UT (trigger 294385), on 2008 March 15 at 15:54:45 UT (trigger 306379; Barthelmy et al. 2008) and on 2009 May 6 at 14:03:27 UT (trigger 351323; Romano et al. 2009d). In the first two instances, *Swift* did not perform a slew, so no narrow-field instrument observations are available.

During the flare of 2009 May 6, the subject of this paper, *Swift* executed an immediate slew, so that the XRT could begin observing the field of SAX J1818.6−1703 about 132 s after the BAT trigger. The automated target (AT) observation lasted for one orbit (until approximately 2300 s after the trigger). Follow-up target of opportunity (ToO) observations for 10 ks were obtained by means of a Cycle 5 proposal (PI, P. Romano; sequences 00031409001–005, see Table 1) and regular ToO observations (00031409006–010). The data cover the first 14 d since the beginning of the outburst.

The BAT data were analysed using the standard BAT analysis software distributed within FTOOLS. Mask-tagged BAT light curves were created in the standard four energy bands, 15–25, 25–50, 50–100 and 100–150 keV, and rebinned to achieve a signal-to-noise ratio (S/N) of 10 (see Figs 1c and d). BAT mask-weighted spectra were extracted from event files over the time interval simultaneous with XRT/Windowed Timing (WT) data (see Table 1) and were rebinned to a S/N of 3. Response matrices were generated with BATDRMGEN. For our spectral fitting (XSPEC v11.3.2) we applied an energy-dependent systematic error. Furthermore, survey data products, in the form of Detector Plane Histograms (DPH) with typical integration time of ∼300 s, are available, and were also analysed with the standard BAT software.

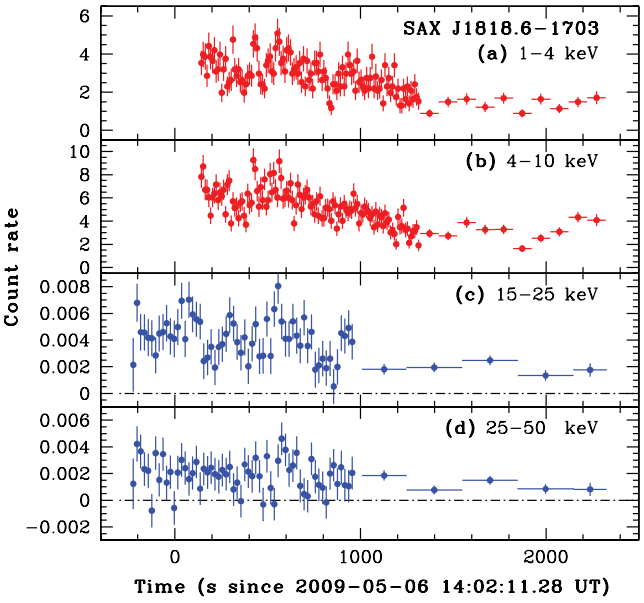

Figure 1. XRT and BAT light curves of the 2009 May 6 outburst in units of count s^{-1} and count s^{-1} detector^{-1}, respectively, showing data collected through the AT observation. The finer sampling points correspond to XRT/WT data (panels a and b) and BAT data in event mode (panels c and d); the remainder are in XRT/PC data and survey mode BAT data.

The XRT data were processed with standard procedures (XRTPIPELINE v0.12.1), filtering and screening criteria by using FTOOLS in the HEASOFT package (v.6.6.1). We considered both WT and PC data, selected event grades 0–2 and 0–12, respectively (Burrows et al. 2005). We corrected for pile-up when appropriate by determining the size of the point spread function (PSF) core affected by comparing the observed and nominal PSF (Romano et al. 2006; Vaughan et al. 2006), and excluding from the analysis all the events that fell within that region. To account for the background, we also extracted events within source-free regions. Exposure maps were generated with the task XRTEXPOMAP. Ancillary response files were generated with XRTMKARF, to account for different extraction regions,

Table 1. Summary of the *Swift* observations.

Sequence	Obs/mode	Start time (UT) (yyyy-mm-dd hh:mm:ss)	End time (UT) (yyyy-mm-dd hh:mm:ss)	Exposure (s)	Time since trigger (s)
00351323000	BAT/event	2009-05-06 13:58:16	2009-05-06 14:18:18	1202	−239
00351323000	BAT/survey	2009-05-06 14:19:03	2009-05-06 14:57:42	1319	1008
00351323000	XRT/WT	2009-05-06 14:04:32	2009-05-06 14:24:15	1183	138
00351323000	XRT/PC	2009-05-06 14:24:17	2009-05-06 14:40:57	977	1322
00031409001	XRT/PC	2009-05-06 15:37:42	2009-05-06 23:44:34	9859	5728
00031409002	XRT/PC	2009-05-07 15:45:00	2009-05-07 18:02:12	4924	92 565
00031409003	XRT/WT	2009-05-08 01:41:00	2009-05-08 17:44:02	168	128 325
00031409003	XRT/PC	2009-05-08 01:41:11	2009-05-08 17:48:57	4782	128 336
00031409004	XRT/PC	2009-05-09 03:13:50	2009-05-09 17:46:57	5919	220 296
00031409005	XRT/PC	2009-05-10 06:30:43	2009-05-10 09:48:41	928	318 508
00031409006	XRT/PC	2009-05-15 21:43:43	2009-05-15 21:54:58	665	805 289
00031409007	XRT/PC	2009-05-16 13:30:33	2009-05-16 15:14:57	1083	862 099
00031409008	XRT/PC	2009-05-17 20:24:37	2009-05-17 22:10:58	1783	973 343
00031409009	XRT/PC	2009-05-18 15:34:27	2009-05-18 17:13:57	1722	1042 332
00031409010	XRT/PC	2009-05-19 15:34:28	2009-05-19 17:20:57	1899	1128 734

vignetting and PSF corrections. We used the spectral redistribution matrices v011 in CALDB.

All quoted uncertainties are given at 90 per cent confidence level for one interesting parameter unless otherwise stated. The spectral indices are parametrized as $F_\nu \propto \nu^{-\alpha}$, where F_ν (erg cm^{-2} s^{-1} Hz^{-1}) is the flux density as a function of frequency ν; we adopt $\Gamma = \alpha + 1$ as the photon index, $N(E) \propto E^{-\Gamma}$ (ph cm^{-2} s^{-1} keV^{-1}). Times in the light curves and the text are referred to as the trigger time.

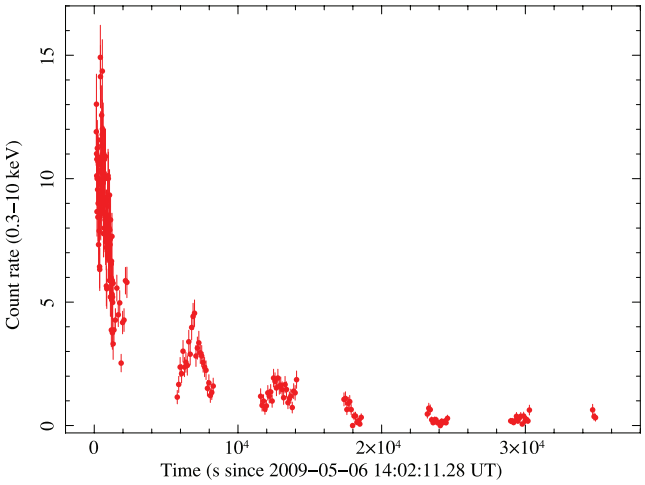

Figure 2. *Swift*/XRT light curve of SAX J1818.6−1703 in the energy range 0.3–10 keV, on a linear scale, during the first day of the bright outburst, showing data collected through both AT and GI ToO observations.

3 RESULTS

Fig. 1 shows the light curves during the brightest part of the outburst in different energy bands. While the BAT count rate was fairly constant throughout the AT observation, the XRT count rate shows a decreasing trend from a maximum of ∼15 counts s^{-1} (in the 0.2–10 keV band; see Fig. 2) with several flares superimposed. The X-ray decreasing trend is even more evident in Fig. 2, which shows the XRT light curve in the 0.3–10 keV band on a linear scale throughout the first day (AT and GI ToO) of observations. The XRT decay time during the first day of the outburst can be fitted with an exponential function, with e-folding time, τ_e, of 3800 ± 100 s. Note, however, that this gives only an idea of the general trend, on top of a lot of short-term variability.

The XRT spectra of the first six temporal sequences reported in Table 1 have been analysed separately to search for variability of the spectral parameters along the bright phase of the outburst. The remaining sequences only provided 3σ upper limits. In Table 2, we report the spectroscopy results obtained when fitting the spectra with simple models, an absorbed power law or blackbody (BB). More complex deconvolutions of the 1–10 keV spectra are not required by the data. No spectral variability is evident, within the large uncertainties.

We extracted simultaneous BAT and XRT spectra between 138 and 937 s since the BAT trigger and performed a joint fit in the 1–10 and 14–150 keV energy bands for XRT and BAT, respectively. A constant factor was included to allow for normalization uncertainties between the two instruments (always resulted within the usual range). The X-ray spectrum is highly absorbed ($N_H \sim 5$–7×10^{22} cm^{-2}) and is very well fitted with models we already adopted to describe other SFXTs wide-band spectra (Sidoli et al. 2009a): power laws with high-energy cut-offs (CUT-OFFPL in XSPEC)

Table 2. XRT spectroscopy.

Sequence	Power law N_H (10^{22} cm^{-2})	Γ	Unabsorbed flux[a] (1–10 keV)	χ^2_{red}/d.o.f. (since trigger)	Times
00351323000 WT	$7.9^{+0.6}_{-0.6}$	$1.1^{+0.1}_{-0.1}$	$1.9^{+0.1}_{-0.1} \times 10^{-9}$	1.0/329	138–1320
00351323000 PC	$9.6^{+2.1}_{-1.8}$	$1.1^{+0.4}_{-0.3}$	$1.3^{+0.2}_{-0.1} \times 10^{-9}$	1.0/50	1322–2299
00031409001 PC	$8.1^{+1.0}_{-0.9}$	$1.7^{+0.2}_{-0.2}$	$3.3^{+0.4}_{-0.3} \times 10^{-10}$	0.8/112	5728–34923
00031409002 PC	$11.0^{+3.3}_{-2.5}$	$1.9^{+0.6}_{-0.5}$	$5.4^{+2.9}_{-5.4} \times 10^{-11}$	0.7/24	92 565–10 0780
00031409003 WT	$7.2^{+1.9}_{-1.6}$	$1.9^{+0.5}_{-0.5}$	$9.7^{+0.7}_{-2.0} \times 10^{-10}$	0.9/23	128 325–186 108
00031409003 PC	$8.1^{+1.4}_{-1.2}$	$1.5^{+0.3}_{-0.3}$	$2.7^{+0.3}_{-0.3} \times 10^{-10}$	0.7/61	128 336–186 388
00031409004 PC	$8.7^{+2.2}_{-1.7}$	$1.4^{+0.4}_{-0.3}$	$1.5^{+0.3}_{-0.8} \times 10^{-10}$	0.9/46	220 296–272 679
00031409005 PC	$9.8^{+7.1}_{-1.3}$	$0.9^{+1.6}_{-1.3}$	$5.7^{+0.8}_{-5.7} \times 10^{-11}$	0.7/5	318 508–330 367
	BB				
Sequence	N_H (10^{22} cm^{-2})	kT (keV)	Unabsorbed flux[a] (1–10 keV)	χ^2_{red}/d.o.f.	R_{BB} (km)[b]
00351323000 WT	$4.8^{+0.4}_{-0.4}$	$2.1^{+0.1}_{-0.1}$	$1.4^{+0.1}_{-0.1} \times 10^{-9}$	1.0/329	$0.8^{+0.1}_{-0.1}$
00351323000 PC	$6.4^{+1.4}_{-1.2}$	$2.1^{+0.3}_{-0.3}$	$9.3^{+0.2}_{-0.1} \times 10^{-10}$	1.0/50	$0.6^{+0.2}_{-0.1}$
00031409001 PC	$4.7^{+0.6}_{-0.5}$	$1.6^{+0.1}_{-0.1}$	$2.0^{+0.1}_{-0.1} \times 10^{-10}$	0.8/112	$0.4^{+0.1}_{-0.1}$
00031409002 PC	$6.6^{+2.2}_{-1.7}$	$1.6^{+0.3}_{-0.2}$	$2.3^{+0.8}_{-0.8} \times 10^{-11}$	0.7/24	$0.2^{+0.1}_{-0.1}$
00031409003 WT	$4.0^{+1.2}_{-1.0}$	$1.4^{+0.2}_{-0.2}$	$5.2^{+0.3}_{-0.1} \times 10^{-10}$	1.0/23	$0.9^{+0.4}_{-0.2}$
00031409003 PC	$4.9^{+0.9}_{-0.8}$	$1.8^{+0.2}_{-0.2}$	$1.7^{+0.3}_{-0.5} \times 10^{-10}$	0.9/61	$0.4^{+0.1}_{-0.2}$
00031409004 PC	$5.2^{+1.3}_{-1.1}$	$1.8^{+0.2}_{-0.2}$	$9.7^{+0.3}_{-0.3} \times 10^{-11}$	0.8/46	$0.3^{+0.1}_{-0.1}$
00031409005 PC	$6.7^{+4.8}_{-3.8}$	$2.2^{+3.7}_{-0.9}$	$4.2^{+2.4}_{-4.2} \times 10^{-11}$	0.8/5	<0.3

[a]Fluxes (corrected for the absorption) are in units of erg cm^{-2} s^{-1}.
[b]BB radii are in units of km, assuming the optical counterpart distance of 2.5 kpc.

Table 3. Spectral fits of simultaneous XRT and BAT data of SAX J1818.6−1703.

Model	Parameters							
CUT-OFFPL	$N_{\rm H}$ [a]	Γ	$E_{\rm cut}$ [b]				Flux[c]	χ^2_ν/d.o.f.
	$6.7^{+0.7}_{-0.7}$	$0.3^{+0.2}_{-0.2}$	$9.1^{+2.4}_{-1.7}$				$4.8^{+0.1}_{-0.1}$	1.0/263
BMC*highecut	$N_{\rm H}$ [a]	$kT_{\rm BB}$ [b,d]	α[d]	log (A)[d]	$E_{\rm cut}$ [b]	$E_{\rm fold}$ [b]	Flux[c]	χ^2_ν/d.o.f.
	$5.3^{+0.3}_{-0.3}$	$1.7^{+0.3}_{-0.3}$	$1.2^{+0.2}_{-1.2}$	$5.7^{+2.3}_{-13.7}$	23^{+5}_{-8}	20^{+10}_{-14}	$4.2^{+0.1}_{-0.1}$	1.0/260
OMPTT[e]	$N_{\rm H}$ [a]	kT_0[b]	kT_e [b]	τ			Flux[c]	χ^2_ν/d.o.f.
	$4.5^{+0.6}_{-0.5}$	$1.4^{+0.1}_{-1.0}$	$6.2^{+0.6}_{-1.1}$	10^{+5}_{-1}			$4.6^{+0.5}_{-1.8}$	1.0/262

[a]Absorbing column density is in units of 10^{22} cm^{-2}.
[b]High-energy cut-off ($E_{\rm cut}$), electron temperature (kT_e), seed photons temperature (kT_0) and the BB colour temperature $kT_{\rm BB}$ are all in units of keV.
[c]Unabsorbed 1–100 keV flux is in units of 10^{-9} erg cm^{-2} s^{-1}.
[d]$kT_{\rm BB}$ is the BB colour temperature of the seed photons, α is the spectral index and Log(A) is the illumination parameter.
[e]Assuming a spherical geometry.

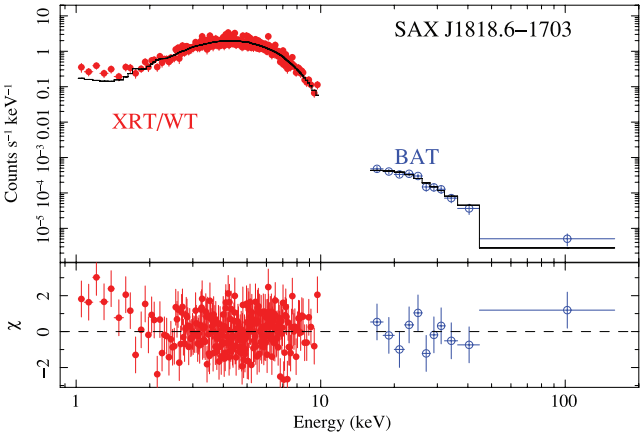

Figure 3. Spectroscopy of the 2009 May 6 outburst. Top: simultaneous XRT/WT (filled red circles) and BAT (empty blue circles) data fitted with an absorbed Comptonization emission (BMC model in XSPEC). Bottom: the residuals of the fit (in units of standard deviations).

or Comptonization models [COMPTT (Titarchuk 1994) or the BMC model (Titarchuk, Mastichiadis & Kylafis 1996) in XSPEC]. The results of the broad-band spectroscopy are summarized in Table 3 (also see Fig. 3).

The BMC model is composed of a BB and its Comptonization, and it is not limited to the thermal Comptonization case (COMPTT) but also can account for dynamical (bulk) Comptonization due to the converging flow. The spectral parameters of the BMC model are the BB colour temperature, $kT_{\rm BB}$, the spectral index α (overall Comptonization efficiency related to an observable quantity in the photon spectrum of the data) and the logarithm of the illuminating factor A, log A (an indication of the fraction of the up-scattered BB photons with respect to the BB seed photons directly visible). In SAX J1818.6−1703 log A could not be constrained, and α was only determined with large uncertainties. Adopting the COMPTT model, the properties of the Comptonizing corona could be constrained well with an electron temperature $kT_{\rm e}$ ∼5–7 keV and an optical depth τ ∼10 (in a spherical geometry).

For the timing analysis we only used the XRT observations in which the source was significantly detected. After correcting the photon arrival times to the Solar system barycentre, we extracted the source events with the same selection criteria used for the spectroscopy. We searched each single data set for coherent suborbital pulsations down to a minimum period corresponding to the Nyquist limit (3.532 ms and 5.0146 s for the data collected in WT and in PC modes, respectively) using the Z^2_n test (Buccheri et al. 1983), with the number of harmonics n being varied from 1 to 4. The period search step size was chosen in each data set in order to oversample the Fourier period resolution ($\frac{1}{2}P^2/T_{\rm obs}$) by a factor of 5. No statistically significant signal was detected. The upper limit on the pulsed fraction (defined as the semi-amplitude of the sinusoidal modulation divided by the mean count rate), computed according to Vaughan et al. (1994), is 12 per cent at the 99 per cent confidence level and for periods between 3.5 ms and 200 s. In order to search for pulsed signals at long periods ($P > 200$ s), we analysed together all the data by computing a Lomb–Scargle periodogram (Scargle 1982). Again, we did not detect any significant signal for periods up to ∼1000 s, with an upper limit on the pulsed fraction of about 25 per cent (at the 99 per cent confidence level).

4 DISCUSSION

SAX J1818.6−1703 is one of the four SFXTs where a period, very likely of orbital origin, has been detected ($P_{\rm orb}$). Such periods have been so far determined either through observations of periodically recurrent outbursts [IGR J11215–5952, Sidoli, Paizis & Mereghetti (2006), Romano et al. (2009c); $P_{\rm orb} \sim 165$ d] or through a timing analysis of the available hard X-ray data [IGR J18483–0311, Sguera et al. (2007), $P_{\rm orb} \sim 18.5$ d; IGR J16479–4514, Jain, Paul & Dutta (2009), $P_{\rm orb} \sim 3.3$ d]. For a fifth SFXT, IGR J08408–4503, we inferred an orbital period of ∼35 d from the times of the outbursts and the duration of the flares (Romano et al. 2009a).

The SAX J1818.6−1703 orbital period of 30 d has been independently obtained by Bird et al. (2009) and by Zurita Heras & Chaty (2009). Assuming as orbital phase zero the same as Bird et al. (MJD 54540.659), the outburst we analyse here (BAT trigger start time) occurred at orbital phase $\phi = 0.90 \pm 0.05$ (1σ error), consistent with the folded light curve and the 4–6 d outburst duration reported by both authors. The new outburst from SAX J1818.6−1703 we are reporting here indeed lasted about 5 d (see Fig. 4), which is also similar to the one in other SFXTs we have been monitoring in the last year with *Swift* (Sidoli et al. 2009a; Romano et al. 2009b) and to the outburst duration in IGR J11215–5952 (Romano et al. 2007).

After the BAT trigger, the whole outburst evolution and the decline phase could be monitored with *Swift*/XRT. The source displays a dynamical range of more than 3000 (see Fig. 4) and a multiple-flaring behaviour previously seen in other SFXTs (Romano et al.

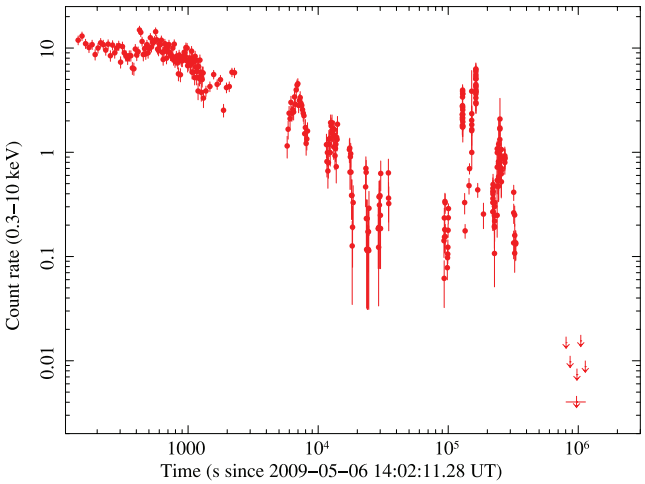

Figure 4. *Swift*/XRT light curve of SAX J1818.6−1703 in the energy range 0.3–10 keV, during the whole campaign. The 4-d gap before the 3σ upper limits is due to the source being Moon constrained. The data shown were collected through both AT and GI ToO, and regular ToO observations.

2009a). The temporally resolved spectroscopy with XRT did not result in variability of the spectral parameters in the 1–10 keV range, within the uncertainties, except for the obvious change in the BB radius, when fitting the soft X-rays with a single absorbed BB (see Table 2). No variability in the absorbing column density could be detected along the outburst, within the uncertainties.

For the first time, we obtained broad-band spectroscopy from soft to hard X-rays of this SFXT, allowing us to compare it with wide-band spectra from a few other SFXTs. Indeed, although SAX J1818.6−1703 has been observed with *INTEGRAL* (Sguera et al. 2005) in the past, only the high-energy part was available (>20 keV) from the IBIS instrument, and the source spectrum has not been obtained (probably because of the low statistics). The *Swift*/XRT and BAT joint simultaneous spectrum during the SAX J1818.6−1703 outburst could be fit very well with a cut-off power law (CUT-OFFPL in XSPEC) or with Comptonized emission models. It is highly absorbed, shows a flat power law (photon index in the range 0.1–0.5) and displays a cut-off constrained between 7 and ∼12 keV (Table 3). The use of the COMPTT model quantifies the physical conditions of the Comptonizing plasma, resulting in a temperature kT_e (5–7 keV) for the Comptonizing plasma and the optical depth τ of the spherical corona ($\tau \sim 10$). The 1–100 keV luminosity is 3×10^{36} erg s^{-1} (assuming 2.5 kpc; Negueruela & Schurch 2007). These SAX J1818.6−1703 broad-band properties are reminiscent of the X-ray spectral shape of the prototype of the SFXT class, XTE J1739–302 (Sidoli et al. 2009b; Sidoli et al. 2009a). The two sources indeed display a similarly high absorption, similar X-ray luminosities, energy cut-off values and hot seed photon temperatures, kT_0, of 1.3–1.4 keV. These spectral parameters indicate the presence of a cold and optically thick corona, which is also similar to that observed in bright neutron star low-mass X-ray binaries (Paizis et al. 2006). No statistically significant pulsations have been found in the *Swift*/XRT data.

The duration of the outbursts, about 5 d, is also similar to the one observed in other SFXTs we have been monitoring last year with *Swift* (Romano et al. 2009b; Sidoli et al. 2009a) and to the outburst duration in IGR J11215–5952 (Romano et al. 2007). All these observed properties, together with the broad-band spectrum we observe now for the first time, confirm the fact that SAX J1818.6−1703 belongs to the class of SFXTs.

ACKNOWLEDGMENTS

We thank the *Swift* team duty scientists and science planners. We also thank the remainder of the *Swift* XRT and BAT teams, S. Barthelmy in particular, for their invaluable help and support. This work was supported in Italy by contracts ASI I/088/06/0 and I/023/05/0, at PSU by NASA contract NAS5-00136. HAK was supported by the *Swift* project.

REFERENCES

Barthelmy S. D., Krimm H. A., Markwardt C. B., Palmer D. M., Ukwatta T. N., 2008, GRB Coordinates Network, 7419, 1
Bird A. J., Bazzano A., Hill A. B. et al., 2009, MNRAS, 393, L11
Bozzo E., Campana S., Stella L. et al., 2008, Astron. Tel., 1493, 1
Buccheri R., Bennett K., Bignami G. F. et al., 1983, A&A, 128, 245
Burrows D. N., Hill J. E., Nousek J. A. et al., 2005, Space Sci. Rev., 120, 165
Grebenev S. A., Sunyaev R. A., 2005, Astron. Lett., 31, 672
Grebenev S. A., Sunyaev R. A., 2008, Astron. Tel., 1482, 1
in't Zand J., Heise J., Smith M. et al., 1998, IAU Circ., 6840, 2
in't Zand J., Jonker P., Mendez M., Markwardt C., 2006, Astron. Tel., 915, 1
Jain C., Biswajit P., Dutta A., 2009, MNRAS, 397, L11
Negueruela I., Schurch M. P. E., 2007, A&A, 461, 631
Negueruela I., Smith D. M., 2006, Astron. Tel., 831, 1
Negueruela I., Smith D. M., Harrison T. E., Torrejón J. M., 2006, ApJ, 638, 982
Paizis A. et al., 2006, A&A, 459, 187
Romano P., Campana S., Chincarini G. et al., 2006, A&A, 456, 917
Romano P., Sidoli L., Mangano V., Mereghetti S., Cusumano G., 2007, A&A, 469, L5
Romano P., Sidoli L., Mangano V. et al., 2008, ApJ, 680, L137
Romano P., Sidoli L., Cusumano G. et al., 2009a, MNRAS, 392, 45
Romano P., Sidoli L., Cusumano G. et al., 2009b, MNRAS, in press (arXiv:0907.1289)
Romano P., Sidoli L., Cusumano G. et al., 2009c, ApJ, 696, 2068
Romano P., Sidoli L., Krimm H. A. et al., 2009d, Astron. Tel., 2044, 1
Scargle J. D., 1982, ApJ, 263, 835
Sguera V., Barlow E. J., Bird A. J. et al., 2005, A&A, 444, 221
Sguera V., Hill A. B., Bird A. J. et al., 2007, A&A, 467, 249
Sidoli L., 2009, Adv. Space Res., 43, 1464
Sidoli L., Paizis A., Mereghetti S., 2006, A&A, 450, L9
Sidoli L., Romano P., Mangano V. et al., 2008, ApJ, 687, 1230
Sidoli L., Romano P., Ducci L. et al., 2009a, MNRAS, 397, 1528
Sidoli L., Romano P., Mangano V. et al., 2009b, ApJ, 690, 120
Titarchuk L., 1994, ApJ, 434, 570
Titarchuk L., Mastichiadis A., Kylafis N. D., 1996, A&AS, 120, C171
Vaughan B. A., van der Klis M., Wood K. S. et al., 1994, ApJ, 435, 362
Vaughan S., Goad M. R., Beardmore A. P. et al., 2006, ApJ, 638, 920
Zurita Heras J. A., Chaty S., 2009, A&A, 493, L1

This paper has been typeset from a TEX/LATEX file prepared by the author.